



# **NAVAL POSTGRADUATE SCHOOL**

**MONTEREY, CALIFORNIA**

## **THESIS**

**THE EFFECTS OF DOUBLE DIFFUSION AND  
BACKGROUND TURBULENCE ON THE PERSISTENCE  
OF SUBMARINE WAKES**

by

Troy A. Benbow

March 2016

Thesis Advisor:  
Second Reader:

Timour Radko  
John Joseph

**Approved for public release; distribution is unlimited**

THIS PAGE INTENTIONALLY LEFT BLANK

<b>REPORT DOCUMENTATION PAGE</b>			<i>Form Approved OMB No. 0704-0188</i>	
Public reporting burden for this collection of information is estimated to average 1 hour per response, including the time for reviewing instruction, searching existing data sources, gathering and maintaining the data needed, and completing and reviewing the collection of information. Send comments regarding this burden estimate or any other aspect of this collection of information, including suggestions for reducing this burden, to Washington headquarters Services, Directorate for Information Operations and Reports, 1215 Jefferson Davis Highway, Suite 1204, Arlington, VA 22202-4302, and to the Office of Management and Budget, Paperwork Reduction Project (0704-0188) Washington, DC 20503.				
<b>1. AGENCY USE ONLY</b> (Leave blank)	<b>2. REPORT DATE</b> March 2016	<b>3. REPORT TYPE AND DATES COVERED</b> Master's thesis		
<b>4. TITLE AND SUBTITLE</b> THE EFFECTS OF DOUBLE DIFFUSION AND BACKGROUND TURBULENCE ON THE PERSISTENCE OF SUBMARINE WAKES			<b>5. FUNDING NUMBERS</b>	
<b>6. AUTHOR(S)</b> Troy A. Benbow				
<b>7. PERFORMING ORGANIZATION NAME(S) AND ADDRESS(ES)</b> Naval Postgraduate School Monterey, CA 93943-5000			<b>8. PERFORMING ORGANIZATION REPORT NUMBER</b>	
<b>9. SPONSORING /MONITORING AGENCY NAME(S) AND ADDRESS(ES)</b> N/A			<b>10. SPONSORING / MONITORING AGENCY REPORT NUMBER</b>	
<b>11. SUPPLEMENTARY NOTES</b> The views expressed in this thesis are those of the author and do not reflect the official policy or position of the Department of Defense or the U.S. Government. IRB Protocol number ____N/A____.				
<b>12a. DISTRIBUTION / AVAILABILITY STATEMENT</b> Approved for public release; distribution is unlimited			<b>12b. DISTRIBUTION CODE</b> A	
<b>13. ABSTRACT (maximum 200 words)</b>  A numerical study has been performed to investigate the feasibility of hydro-dynamically based detection of propagating submersibles. Of particular concern is the possibility of utilizing microstructure measurements as a means of wake identification. The simulations are based on the Massachusetts Institute of Technology General Circulation Model (MITgcm), which has been modified for wake analysis. The dissipation of a turbulent wake produced by a sphere uniformly propagating in a doubly stratified environment is examined for three scenarios: (i) quiescent regime, (ii) double-diffusive regime, and (iii) a flow with pre-existing turbulence. The analysis of the numerical models was based on two quantities, the dissipation of turbulent kinetic energy ( $\epsilon$ ), and the dissipation of thermal variance ( $\chi$ ). This analysis indicates that wake signatures generated by a 1-meter wide object are detectable for 0.4 and 1.2 hours, depending on regime, and the detection interval is not strongly sensitive to the density ratio. Double-diffusive convection plays a significant role in the duration of submarine wakes. The extrapolation of the simulations to objects of ~10m propagating with speeds ~10m/s suggests that microstructure-based detection is feasible for at least two hours after the passage of a submersible and significantly longer outside the double-diffusive regime. These results indicate that microstructure-based observations of stratified wakes offer a viable method for the non-acoustic detection of submerged objects.				
<b>14. SUBJECT TERMS</b> fluid dynamics, submarine, wakes, turbulence			<b>15. NUMBER OF PAGES</b> 41	
			<b>16. PRICE CODE</b>	
<b>17. SECURITY CLASSIFICATION OF REPORT</b> Unclassified	<b>18. SECURITY CLASSIFICATION OF THIS PAGE</b> Unclassified	<b>19. SECURITY CLASSIFICATION OF ABSTRACT</b> Unclassified	<b>20. LIMITATION OF ABSTRACT</b> UU	

THIS PAGE INTENTIONALLY LEFT BLANK

**Approved for public release; distribution is unlimited**

**THE EFFECTS OF DOUBLE DIFFUSION AND BACKGROUND TURBULENCE  
ON THE PERSISTENCE OF SUBMARINE WAKES**

Troy A. Benbow  
Lieutenant, United States Navy  
B.S., United States Naval Academy, 2008

Submitted in partial fulfillment of the  
requirements for the degree of

**MASTER OF SCIENCE IN PHYSICAL OCEANOGRAPHY**

from the

**NAVAL POSTGRADUATE SCHOOL  
March 2016**

Approved by: Timour Radko  
Thesis Advisor

John Joseph  
Second Reader

Peter Chu  
Chair, Department of Oceanography

THIS PAGE INTENTIONALLY LEFT BLANK

## ABSTRACT

A numerical study has been performed to investigate the feasibility of hydrodynamically based detection of propagating submersibles. Of particular concern is the possibility of utilizing microstructure measurements as a means of wake identification. The simulations are based on the Massachusetts Institute of Technology General Circulation Model (MITgcm), which has been modified for wake analysis. The dissipation of a turbulent wake produced by a sphere uniformly propagating in a doubly stratified environment is examined for three scenarios: (i) quiescent regime, (ii) double-diffusive regime, and (iii) a flow with pre-existing turbulence. The analysis of the numerical models was based on two quantities, the dissipation of turbulent kinetic energy ( $\epsilon$ ), and the dissipation of thermal variance ( $\chi$ ). This analysis indicates that wake signatures generated by a 1-meter wide object are detectable for 0.4 and 1.2 hours, depending on regime, and the detection interval is not strongly sensitive to the density ratio. Double-diffusive convection plays a significant role in the duration of submarine wakes. The extrapolation of the simulations to objects of  $\sim 10\text{m}$  propagating with speeds  $\sim 10\text{m/s}$  suggests that microstructure-based detection is feasible for at least two hours after the passage of a submersible and significantly longer outside the double-diffusive regime. These results indicate that microstructure-based observations of stratified wakes offer a viable method for the non-acoustic detection of submerged objects.

THIS PAGE INTENTIONALLY LEFT BLANK

## TABLE OF CONTENTS

<b>I.</b>	<b>INTRODUCTION.....</b>	<b>1</b>
<b>A.</b>	<b>MOTIVATION AND NAVAL RELEVANCE .....</b>	<b>1</b>
<b>B.</b>	<b>BACKGROUND .....</b>	<b>1</b>
<b>II.</b>	<b>MODEL DEVELOPMENT .....</b>	<b>5</b>
<b>A.</b>	<b>MODEL FUNDAMENTALS.....</b>	<b>5</b>
<b>B.</b>	<b>MODEL PARAMETERS .....</b>	<b>6</b>
<b>C.</b>	<b>FLUID REGIMES .....</b>	<b>8</b>
<b>III.</b>	<b>RESULTS .....</b>	<b>11</b>
<b>A.</b>	<b>ANALYSIS METHODS .....</b>	<b>11</b>
<b>B.</b>	<b>QUIESCENT REGIME .....</b>	<b>12</b>
<b>C.</b>	<b>DOUBLE-DIFFUSIVE REGIME .....</b>	<b>14</b>
<b>D.</b>	<b>PRE-EXISTING TURBULENCE REGIME .....</b>	<b>16</b>
<b>IV.</b>	<b>DISCUSSION .....</b>	<b>19</b>
<b>A.</b>	<b>FLUID REGIME EFFECTS .....</b>	<b>19</b>
<b>B.</b>	<b>DENSITY RATIO EFFECTS.....</b>	<b>19</b>
<b>C.</b>	<b>REAL-WORLD ESTIMATES .....</b>	<b>20</b>
<b>D.</b>	<b>CONCLUSIONS .....</b>	<b>21</b>
	<b>LIST OF REFERENCES .....</b>	<b>23</b>
	<b>INITIAL DISTRIBUTION LIST .....</b>	<b>25</b>

THIS PAGE INTENTIONALLY LEFT BLANK

## LIST OF FIGURES

Figure 1.	Velocity Profiles of Towed and Jet-Propelled Body .....	2
Figure 2.	Schematic of Scales in the Ocean .....	6
Figure 3.	Three-Dimensional Visualization of the Submarine Wake .....	8
Figure 4.	Initial Conditions for Temperature Anomaly in Double-Diffusion Regime .....	9
Figure 5.	Model Simulation Depicting the Different Analysis Areas .....	11
Figure 6.	Difference in Dissipation of Kinetic Energy Created by the Submarine Wake in the Quiescent Regime .....	13
Figure 7.	Difference in Dissipation of Thermal Variance Created by Submarine Wake in the Quiescent Regime .....	14
Figure 8.	Difference in Dissipation of Kinetic Energy Created by the Submarine Wake in the Double-Diffusive Regime .....	15
Figure 9.	Difference in Dissipation of Thermal Variance Created by the Submarine Wake in the Double-Diffusive Regime .....	16
Figure 10.	Difference in Dissipation of Kinetic Energy Created by the Submarine Wake in the Pre-existing Turbulence Regime .....	17
Figure 11.	Difference in Dissipation of Thermal Variance Created by the Submarine Wake in the Pre-existing Turbulence Regime .....	18

THIS PAGE INTENTIONALLY LEFT BLANK

## LIST OF TABLES

Table 1.	Initial Structure of Temperature, Salinity and Density Gradient for the MITgcm Model .....	7
----------	--	---

THIS PAGE INTENTIONALLY LEFT BLANK

## ACKNOWLEDGMENTS

The author would like to acknowledge the contributions of the following individuals, who made the completion of this thesis possible:

Timour Radko, thesis advisor

John Joseph, second reader

Erick Edwards

Jason D. Flanagan

Mario Durán Camejo

University of Texas Advanced Computing Center

Department of Defense High Power Computing Modernization Program

THIS PAGE INTENTIONALLY LEFT BLANK

# **I. INTRODUCTION**

## **A. MOTIVATION AND NAVAL RELEVANCE**

Modern anti-submarine warfare relies heavily on the use of acoustical detection methods to track targets. The widespread proliferation of ultra-quiet, air-independent propulsion submarines with signal-to-noise levels significantly below the threshold of acoustic detection demands new, innovative methods of detection. The dramatic improvement of remote sensing methods enables highly accurate measurements of submarine wakes. This thesis will evaluate the nature of submarine wakes in stratified fluids to enable the effective employment of available technology.

## **B. BACKGROUND**

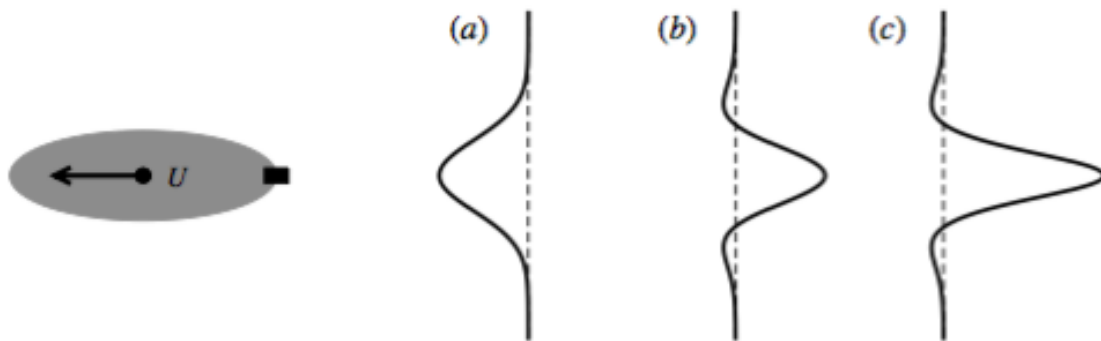
The nature of turbulent wakes has been an area of active scientific investigation. The beginnings of what could be considered modern study of turbulence were experiments conducted by Reynolds into the nature of turbulent flow. Reynolds's research examined the point at which flow transformed from laminar to turbulent, and expressed that relationship as a function of the mean fluid velocity and its viscosity, relative to the size of the flow region (Reynolds Number). If this ratio reaches a critical value, laminar flow will begin to transition to turbulent flow. Another key observation of Reynolds's research was that these critical velocities were susceptible to initial disturbances in the fluid. If these disturbances were large, unstable motion occurred before the critical velocity was reached (Reynolds 1883).

Reynolds's work provided the basis for much of the subsequent research on fully developed turbulence. The manner in which the turbulence dissipates is equally as important as generating it in the first place. Richardson (1926) developed the concept of the energy cascade. The key premise of this cascade was that energy was imparted into a system at large scales, and then it is transferred nonlinearly into a successively smaller and smaller eddies. Kolmogorov (1941) expanded the energy cascade concept. Energy is imparted on the large scale and dissipates on the viscous scale. This import of energy, at sufficiently high Reynolds numbers, generates large scale turbulent eddies (Ecke 2005).

The inertia and viscous forces do not solely influence the turbulence of wakes generated in the ocean. Since the ocean is typically stratified due to variations in density, the wake also experiences gravitational or buoyant forces. The inhibited vertical motion caused by a stratified fluid has a number of influences on a submarine wake. The increase in potential energy (displacement of buoyant water via mixing) induces an equilibrium force. This force causes the vertical component of the wake to collapse and generate internal waves. However, if the ratio of inertial to buoyant forces (Froude number) is sufficiently high, inertial forces dominate and the wake behavior is similar that of a non-stratified fluid. This wake collapse causes the horizontal motion to prevail over the vertical motion creating horizontally unstable conditions that cause meandering horizontal vortices (Lin and Pao 1979).

Modern computing has enabled the use of direct numerical simulations (DNS) to observe turbulent structures of wakes. There are three fundamental types of wakes, each with their own unique characteristics: (a) a dragged body with no propulsion, (b) zero net momentum, and (c) propelled body with excess momentum (Brucker and Sarkar 2010). See Figure 1.

Figure 1. Velocity Profiles of Towed and Jet-Propelled Body



The image shows the fluid velocity behind the moving body shown on the left. a) Dragged body with no propulsion (b) self-propelled body (c) propelled body with excess momentum. The dashed line represents zero velocity. Source: M.B. de Stadler and S. Sarkar, 2011: Simulation of a propelled wake with moderate excess momentum in a stratified fluid. *J. Fluid Mech.*, **692**, 28–52, doi:10.1017/jfm.2011.489.

Discerning the microstructure differences between towed and propelled wakes is non-trivial. All turbulent wakes contain three distinct regions: (i) the initially three-dimensional turbulent range, (ii) an intermediate non-equilibrium range where dissipation of kinetic energy decreases, and finally (iii) a quasi-two-dimensional regime with minimal vertical velocities. Through DNS several key distinctions are noted between wakes of type (a) compared to (b) or (c). In the self-propelled case, larger mean shear transfers more energy to turbulent shear production. The turbulent stress created by the mean shear is mitigated by buoyancy and reduces the turbulence production, particularly in the vertical. This effect is enhanced in stratified self-propelled wakes. As a result, self-propelled wakes persist longer than both unstratified wakes and towed wakes. These buoyancy influences can create anisotropy in the velocity field of the stratified wake (Brucker and Sarkar 2010). Additionally, the type of momentum source, jet, propeller, etc., and the acceleration of the body can also have significant impacts on the structure of the wake (de Stadler and Sarker 2011). These small-scale buoyancy effects are critical to both towed and self-propelled wake structure in stratified fluids. This study specifically investigates how variances in density influence both the buoyant forces present in the microstructure of a submarine wake, and the effect these forces have on the wake duration of a three dimensional axisymmetric body with no propulsion.

One common natural process that influences buoyancy and stratification, both central factors that dictate the nature of submarine wakes, is double-diffusive convection. Favorable conditions for formation of double diffusion occur in 44% of the world's oceans (You 2002). Ninety percent of the Atlantic Ocean has a density ratio less than 2.3. In certain areas of the Atlantic, 95% of the upper kilometer is favorable for salt fingering having density ratios between 1.5 and 2.5 (Schmitt 1994). One of the consequences of active double-diffusion is the formation of thermohaline staircases, which is attributed to variations of the ratio of heat and salt fluxes as a function of density ratio (Radko 2013). While double-diffusive phenomena have been the subject of many DNS, including Naval Postgraduate School research by Ball (2015), their effects on the duration of submarine wakes have not been examined.

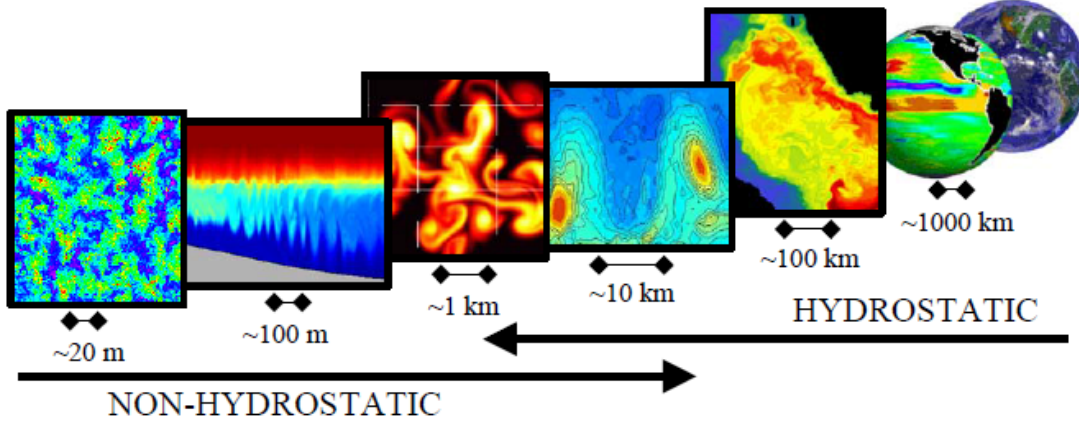
THIS PAGE INTENTIONALLY LEFT BLANK

## **II. MODEL DEVELOPMENT**

### **A. MODEL FUNDAMENTALS**

Oceanic General Circulation models are commonly used to represent the interactions of momentum and buoyancy on a rotating domain. These interactions are accurately described by the Navier-Stokes equations, and their scales occur from thousands of kilometers to centimeters. One of the key features of MITgcm, the model used in the present investigation, is that its algorithms can utilize the incompressible Navier-Stokes equations and subsequently perform over a broad range of scales (Figure 2). The non-hydrostatic capability of MITgcm makes it suitable to accurately analyze the centimeter scale features created by the turbulent wake of a submarine (Marshall et al. 1997). In addition to the robust model physics, MITgcm offers a great deal of flexibility in the structure of the model parameterizations. These calculations require an immense amount of computing power and are only possible through the use of modern super computers such as Cray XE6. This research utilized more than 100,000 computing hours on the Department of Defense High Power Computation Modernization Program and the University of Texas Advanced Computing Center.

Figure 2. Schematic of Scales in the Ocean



Schematic of the relative size of ocean scales indicating the area where hydrostatic dynamics gives way to non-hydrostatic dynamics. Source: A. Adcroft, C. Hill, J. Campin, J. Marshall, and P. Heimbach, 2004: Overview of the Formulation and Numerics of the MIT GCM. *Proc. ECMWF Semin. Ser. Numer. Methods Recent Dev. Numer. methods Atmos. Ocean Model.*, 139–149.

## B. MODEL PARAMETERS

The ideal DNS would be a realistically shaped submarine producing real thrust via its propeller. Unfortunately, the resolution required for accurate measurement of dissipation and the computation power required for that resolution make a real world simulation unfeasible. The solution is to create a simplified and smaller model. In the following simulation, a solid sphere with a 0.6-meter diameter is passed through a rectangular region with x, y, and z scale of 4, 2, and 2 meters, respectively. The surface temperature, 19.92 °C; bottom temperature, 20.0 °C; and surface salinity 35.03 ‰ were constant across all experiments. The density ratio ( $R_\rho$ ) was varied for each model by changing  $ds/dz$  (Table 1). The values of temperature and salinity gradients, as well as the density ratio, were based on typical oceanographic observations where double diffusion is common. No salt fingers are observed when  $R_\rho$  is larger than two. Typical occurrences of salt-finger staircases occur at a  $R_\rho$  less than 1.8 (Radko 2013).

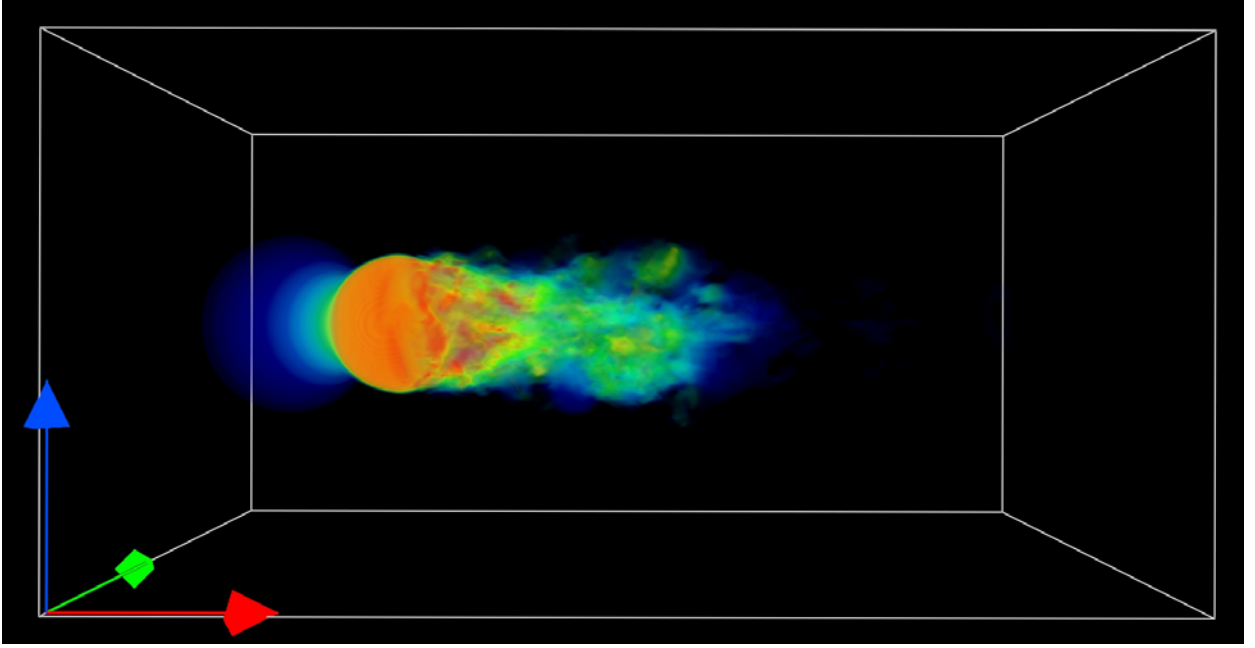
Table 1. Initial Structure of Temperature, Salinity and Density Gradient for the MITgcm Model

$R_p$	Surface Temperature	Bottom Temperature	Surface Salinity	Bottom Salinity	Density Gradient*
1.5	20	19.92	35.03	35.0156	0.00941019
2.0	20	19.92	35.03	35.0192	0.0107835
2.5	20	19.92	35.03	35.0213	0.0115846

\*Values for density gradient were determined based on UNESCO 1983 (EOS 80) polynomial. Source: Ocean Physics Group at Scripps Institute of Oceanography at University of California San Diego, cited December 1, 2015: [http://opgl.ucsd.edu/~sio221/SIO\\_221A\\_2009/SIO\\_221\\_Data/Matlab5/seawater/Values](http://opgl.ucsd.edu/~sio221/SIO_221A_2009/SIO_221_Data/Matlab5/seawater/Values).

In order to attain the highest possible resolution while still having a long-enough model runtime to observe the required features, each model run was divided into three distinct intervals. The first 30 minutes of the model output were saved every 10 seconds, and the time step for each model calculation was 0.025s. From 30–75 minutes, the output was saved every minute with time step of 0.125s. Beyond 75 minutes, the output was saved every 5 minutes with time step of 0.625s. This scheme was developed in order to observe the large amount of turbulence and fine detail induced as the submarine passes through the domain and the immediate aftermath. Afterward, the larger time steps allow observations of several hours. As the wake dissipates, the magnitude of the perturbations and their rates of change become smaller resulting in relevant observations of the microstructure over periods of several hours. Given the computation power required for these calculations this compromise was an important factor in model implementation. These conditions allowed the creation of fully developed turbulent wakes under a variety of conditions (Figure 3)

Figure 3. Three-Dimensional Visualization of the Submarine Wake



A three-dimensional visualization of the submarine wake in the quiescent regime created through the Visualization and Analysis Platform for Ocean, Atmosphere, and Solar Researchers (VAPOR) software. Colors indicate velocity (higher in red, lower in blue). Red, green and blue axes indicate x, y and z-axis, respectively.

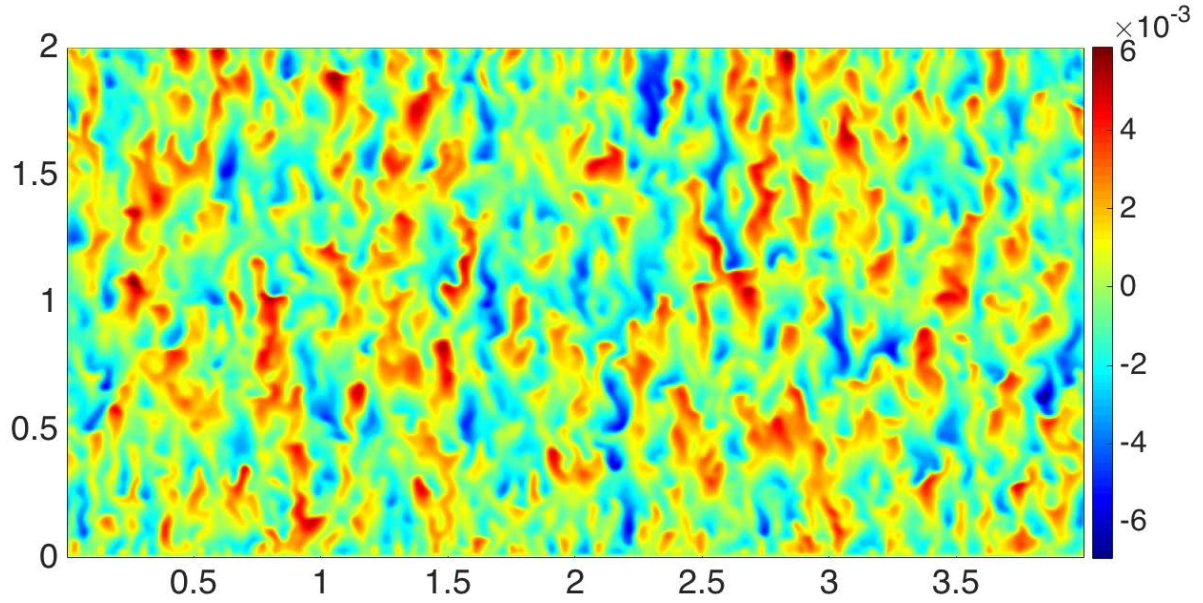
### C. FLUID REGIMES

In order to investigate the spatial and temporal patterns of the submarine wake microstructure, three different model representations were employed. The first and most basic case is an initially calm fluid, with uniform stratification and a constant gradient of both temperature and salinity. Throughout the entire domain, the fluid velocity was initially set to zero. The values of temperature, salinity, and velocity at the surface and bottom boundary vary according to the submarine interactions within the domain. The vertical eddy viscosity coefficient of the model and the Laplacian friction coefficient are set to  $10^{-6} \text{ m}^2\text{s}^{-1}$ . Lateral and vertical eddy diffusivity of salt and temperature ( $K_s$  and  $K_t$ ) both set to  $10^{-6} \text{ m}^2\text{s}^{-1}$ .

The second regime examined the effect that pre-existing salt fingers and active double-diffusive convection have on wake duration. The initial conditions were modified from the quiescent case as follows. The diffusivity of salt  $K_s$  was changed to  $10^{-7} \text{ m}^2\text{s}^{-1}$ .

The time step was changed to 0.5 seconds and the model was run without the submarine for 3.3 hours. This period of integration was sufficient to produce fully developed quasi-equilibrium double-diffusive convection, which was used as an initial condition for the stratified wake experiment (Figure 4). The time step parameters were then reset to the same values as the first experiment and the sub was passed through the domain.

Figure 4. Initial Conditions for Temperature Anomaly in Double-Diffusion Regime



Temperature anomaly depicting double-diffusive salt fingers in an X-Z plane of the model domain at  $y=200$ . X- and Z-axis indicate grid location in meters, while color depicts positive (red) and negative (blue) temperature anomaly in  $^{\circ}\text{C}$  at  $t = 3.33$  hours. This example is for  $R_p = 1.5$

The third regime, pre-existing turbulence, is set up similarly to the double-diffusive case. Once the turbulent salt fingers formed (Figure 4), the value of  $K_s$  was reset to  $10^{-6} \text{ m}^2\text{s}^{-1}$ . The pre-existing regime did not have active double diffusion during the submarine wake formation and dissipation. Varying the diffusivities was an effective way to create small initial perturbations of the same order of magnitude as in typical wave-induced turbulent patches in the ocean.

The surface and bottom boundary conditions of the first regime differed from the second and third. In the quiescent stratified case the values of temperature and salinity

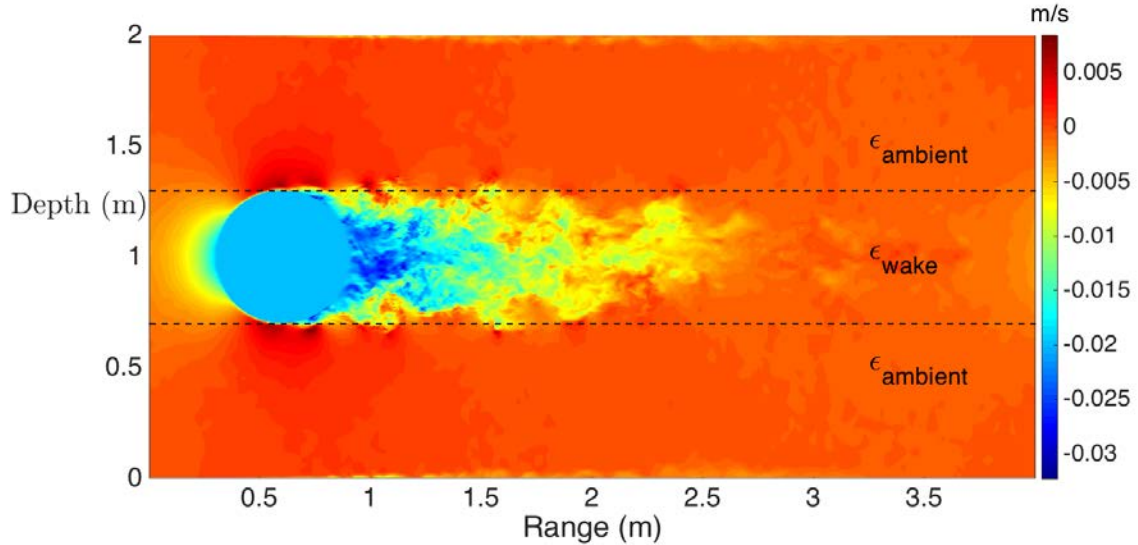
were could vary freely in time as submarine turbulence created variation in the water's temperature, salinity, and velocity. In the double diffusion, and pre-existing turbulence cases the surface and bottom temperature and salinity values were maintained at the same level for the entire duration of the experiment. Over a long-enough period, the entire domain could have become homogenized in distribution of temperature and salinity. Since the typical water column in the ocean would not become fully mixed through wake generation, these boundary conditions ensured that the domain maintained some degree of stratification throughout the time scales used. For each version of the model, (quiescent, double diffusive and turbulent) at least three experiments were performed with different values of density ratio  $R_\rho = 1.5, 2, 2.5$ .

### III. RESULTS

#### A. ANALYSIS METHODS

To analyze the wake duration its signature had to be identifiable from the background noise. Since the majority of turbulence occurs directly behind the submarine, that area was separated from the rest of the model domain, which was divided into three sub-regions. The first region was a 0.6-meter wide area through which the submarine was passed and centered in the domain. The other two regions were 0.6-meter regions on either side of the submarine (Figure 5). An area of 0.10 meters near the surface and bottom boundary was eliminated from the analysis. This is the region where the boundary condition was applied, and omitting these areas eliminated any spurious signal due to increased noise at the boundary.

Figure 5. Model Simulation Depicting the Different Analysis Areas



A two-dimensional slice of the simulation domain in the X-Z plane; 112 seconds elapsed. The three distinct regions for analysis are divided by black dashed lines. The vertical axis and horizontal axis depict gird distance in meters, while colors indicate  $u$  component of velocity.

From model output of temperature, and velocity data, dissipation of kinetic energy ( $\epsilon$ ) and dissipation of thermal variance ( $\chi$ ) were calculated. An x-y mean of ( $\epsilon$ ) and ( $\chi$ ) was calculated creating a one-dimensional profile. With this profile, a difference between  $\epsilon_{\text{ambient}}$  and  $\epsilon_{\text{wake}}$  was evaluated. Once the difference between the submarine wake region and the ambient regions was less than zero, the wake was considered indistinguishable from the background. Based on the direct numerical simulation,  $\epsilon_{\text{wake}}$  becomes indistinguishable from  $\epsilon_{\text{ambient}}$  when both quantities are in the range of  $10^{-13}$  to  $10^{-14} \text{ W kg}^{-1}$ .

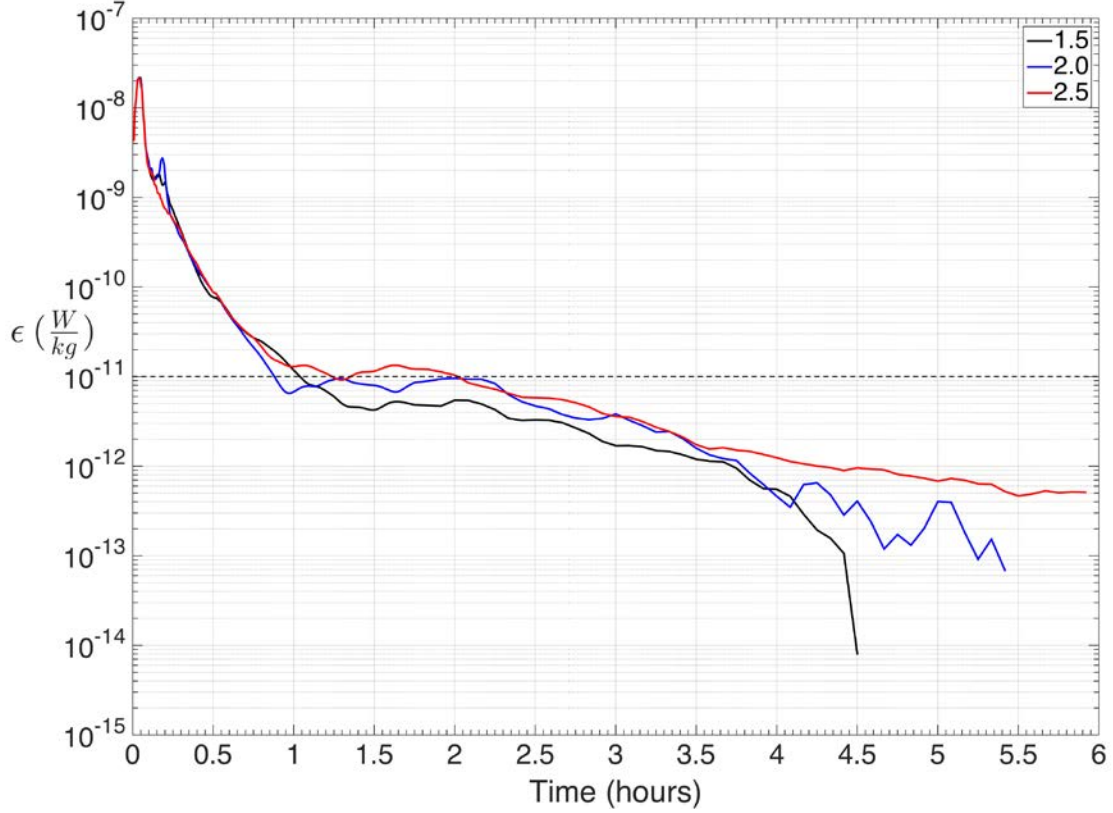
Typical ocean measurements of  $\epsilon$  and  $\chi$  are commonly made using free falling high-resolution profilers; however, profilers on ocean gilders are achieving measurements of similar quality. These gilder-based profilers resolve  $\epsilon$  and  $\chi$  on the order  $10^{-11} \text{ W kg}^{-1}$  (Peterson 2013), and this level will be used as a nominal detection threshold in the analysis of DNS. The results will reference two quantities: (i) the region that is detectable using current measurements, the detection threshold, and (ii) the point at which the signal is fundamentally indistinguishable from the background, total dissipation time.

## B. QUIESCENT REGIME

For  $\epsilon$ ,  $R_p = 2.0$  was the first wake to dissipate below the threshold in 0.8667 hours.  $R_p = 1.5$  reached the detection threshold value in 1.033 hours and  $R_p = 2.5$  followed at 1.233 hours. Total dissipation occurred in 4.5, 5.417 and 5.917 hours for  $R_p = 1.5$ , 2.0, and 2.5, respectively (Figure 6).

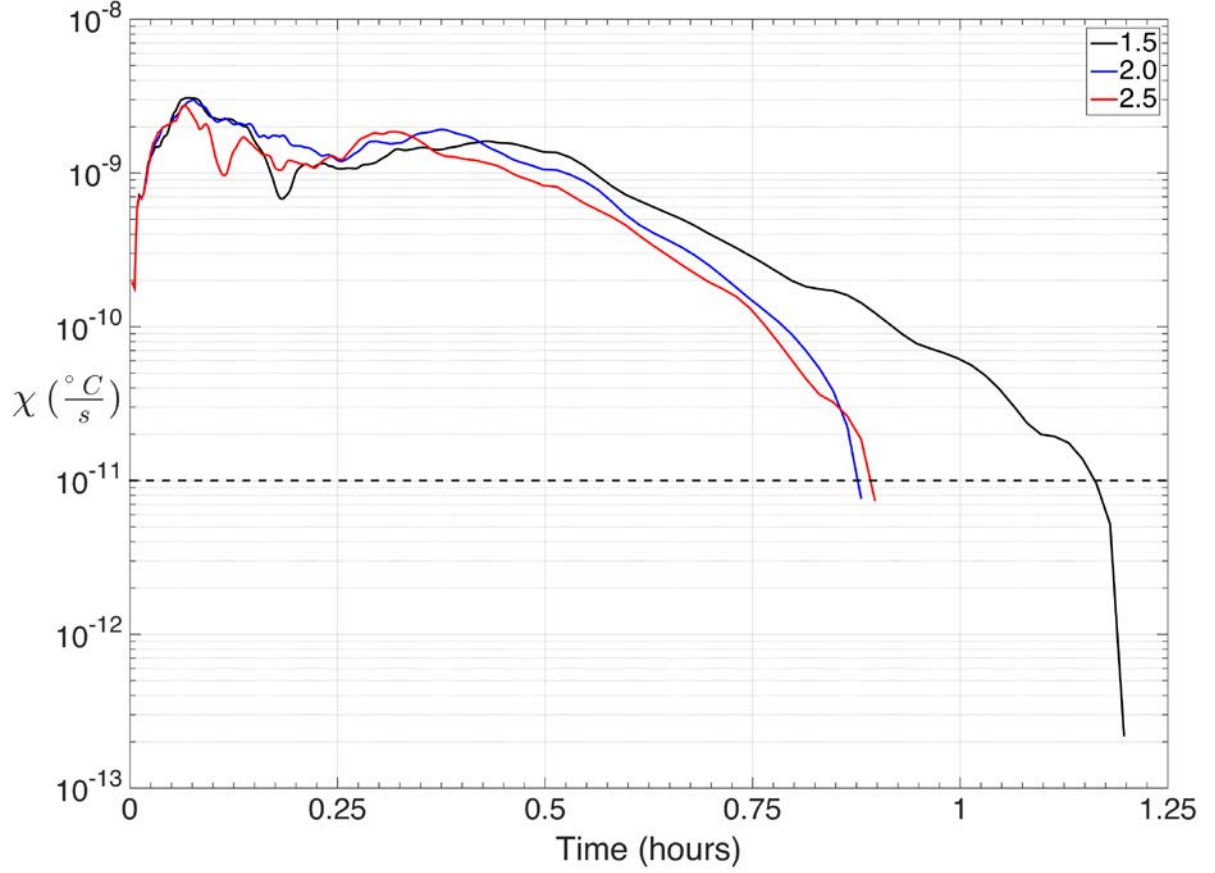
With  $R_p = 2.0$ ,  $\chi$  reached the threshold value in 0.7806 hours and  $R_p = 2.5$  followed in 0.7639 hours.  $R_p = 1.5$  reached the threshold in 0.9139 hours (Figure 7). Unlike  $\epsilon$ , differences in thermal variance did not persist any significant length of time past the detection threshold value.

Figure 6. Difference in Dissipation of Kinetic Energy Created by the Submarine Wake in the Quiescent Regime



Difference in dissipation of kinetic energy for the quiescent regime. The y-axis displays a logarithmic plot of the difference between  $\epsilon_{\text{wake}}$  and  $\epsilon_{\text{ambient}}$  in  $\text{W kg}^{-1}$ . X-axis is measured in hours.  $R_p$  of 1.5, 2.0 2.5 are shown in black, blue and red, respectively. The horizontal black dashed line displays the detection threshold.

Figure 7. Difference in Dissipation of Thermal Variance Created by Submarine Wake in the Quiescent Regime

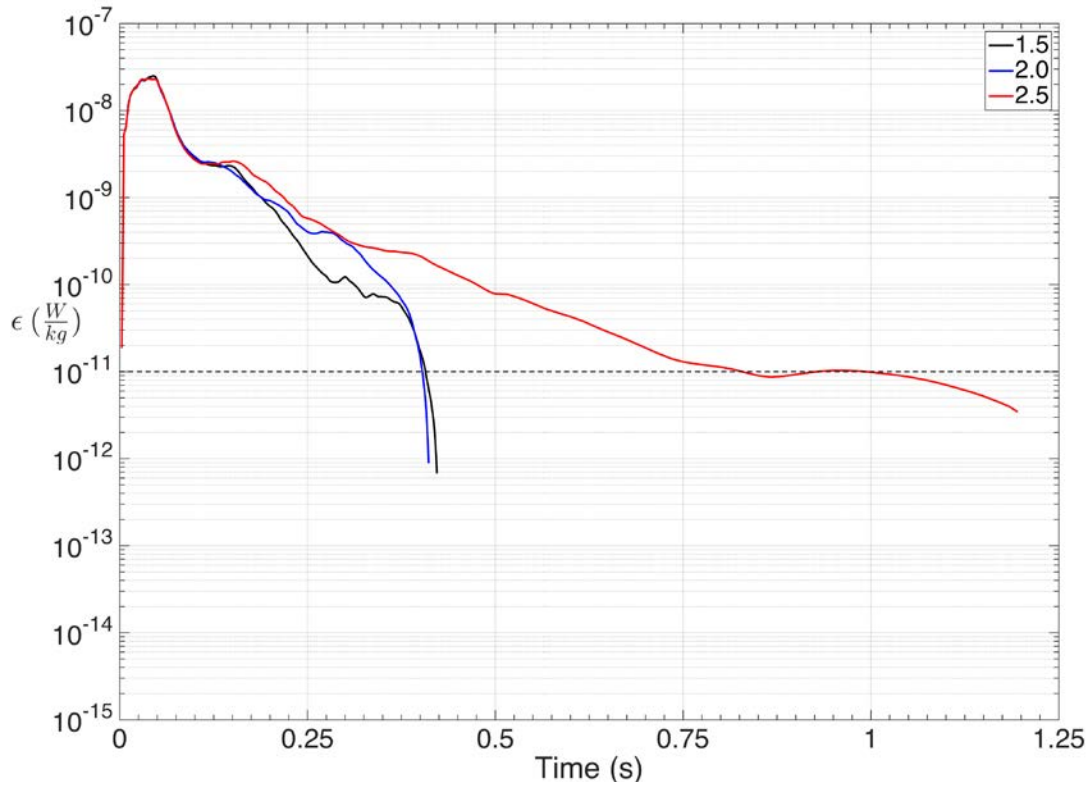


Difference in dissipation of thermal variance for the quiescent regime. The y-axis displays a logarithmic plot of the difference between  $\chi_{\text{wake}}$  and  $\chi_{\text{ambient}}$  in  $^{\circ}\text{C s}^{-1}$ . X-axis is measured in hours.  $R_p$  of 1.5, 2.0 2.5 are shown in black, blue and red, respectively. The horizontal black dashed line displays the detection threshold.

### C. DOUBLE-DIFFUSIVE REGIME

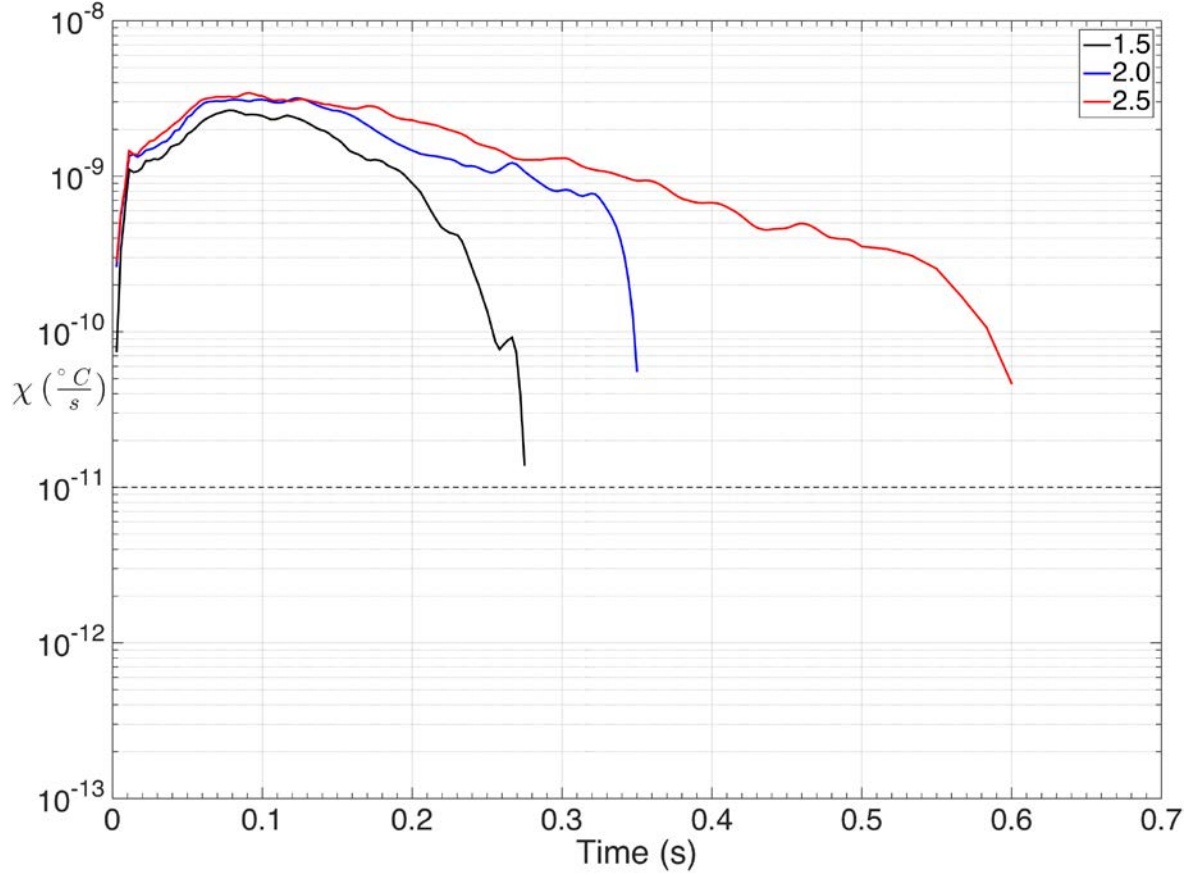
The double-diffusive regime displayed the fastest dissipation across all density ratios.  $R_p = 2.0$  was quickest to reach the threshold value in 0.4029 hours.  $R_p = 1.5$  reached the detection threshold a fraction of a second later in 0.4056 hours.  $R_p = 2.5$  dissipated below the detection threshold in 0.8167 hours (Figure 8). For  $\chi$ , the exact point of the detection threshold was difficult to evaluate because of the low frequency of the model output. The total dissipation times were 0.275, 0.35, and 0.6 hours for  $R_p = 1.5$ , 2.0, and 2.5, respectively (Figure 9) and it can be safely assumed that the detection threshold was reached close to these periods

Figure 8. Difference in Dissipation of Kinetic Energy Created by the Submarine Wake in the Double-Diffusive Regime



Difference in dissipation of kinetic energy for the double-diffusive regime. The y-axis displays a logarithmic plot of the difference between  $\epsilon_{\text{wake}}$  and  $\epsilon_{\text{ambient}}$  in  $^\circ\text{C s}^{-1}$ . X-axis is measured in hours.  $R_p$  of 1.5, 2.0 2.5 are shown in black, blue and red, respectively. The horizontal black dashed line displays the detection threshold

Figure 9. Difference in Dissipation of Thermal Variance Created by the Submarine Wake in the Double-Diffusive Regime



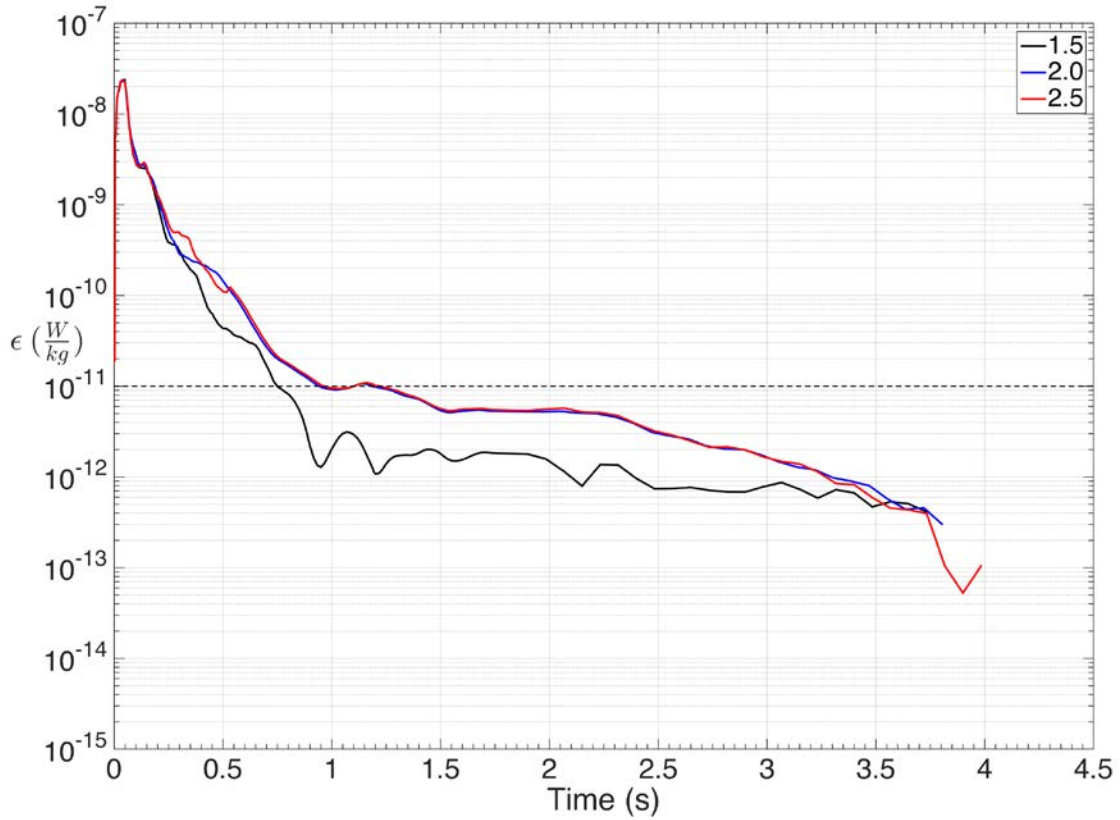
Difference in dissipation of thermal variance for the double-diffusive regime. The y-axis displays a logarithmic plot of the difference between  $\chi_{\text{wake}}$  and  $\chi_{\text{ambient}}$  in  $\text{°C s}^{-1}$ . X-axis is measured in hours.  $R_p$  of 1.5, 2.0 2.5 are shown in black, blue and red, respectively.

#### D. PRE-EXISTING TURBULENCE REGIME

The pre-existing turbulence regime  $R_p = 1.5$  was the fastest to reach the detection threshold; 0.75 hours and the total dissipation time was 3.733 hours.  $R_p = 2.0$  and 2.5 look nearly identical. The wake reached the threshold value at 0.9367 and 0.95 hours and total dissipation occurred at 3.803 and 3.903 hours, respectively (Figure 10).

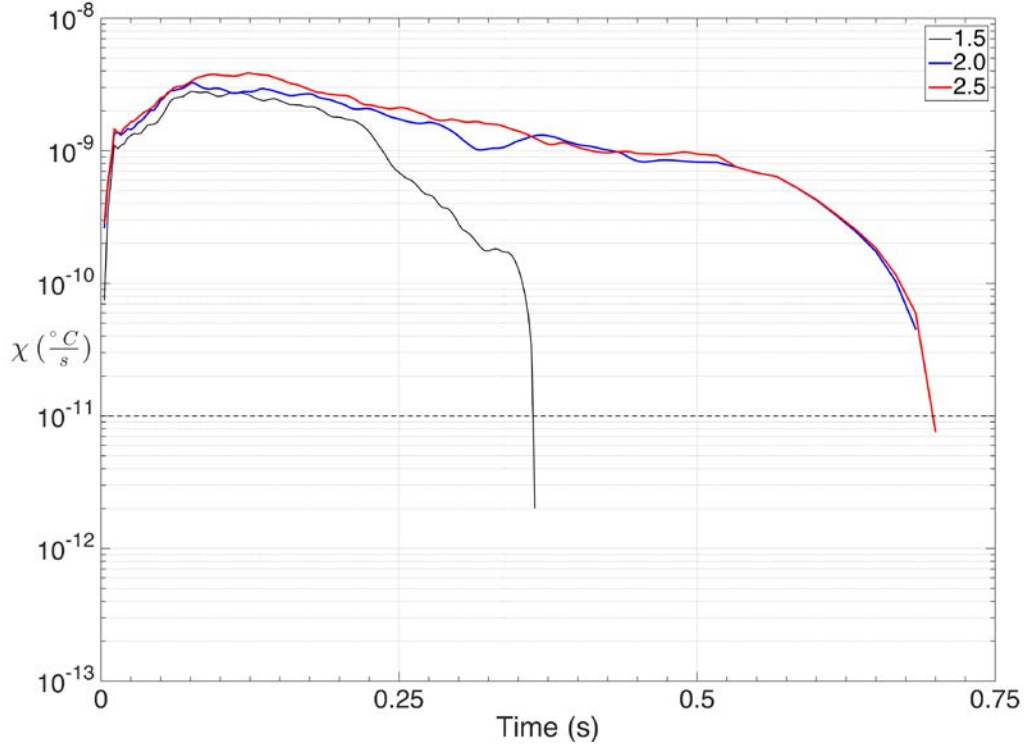
The thermal variance dissipated in 0.3639, 0.6833 and 0.7 hours for  $R_p = 1.5$ , 2.0 and 2.5, respectively, and there was no significant wake remaining below the detection threshold (Figure 11).

Figure 10. Difference in Dissipation of Kinetic Energy Created by the Submarine Wake in the Pre-existing Turbulence Regime



Difference in dissipation of kinetic energy for the pre-existing turbulence regime. The y-axis displays a logarithmic plot of the difference between  $\epsilon_{wake}$  and  $\epsilon_{ambient}$  in  $^{\circ}C \ s^{-1}$ . X-axis is measured in hours.  $R_p$  of 1.5, 2.0 2.5 are shown in black, blue and red, respectively. The horizontal black dashed line displays the detection threshold.

Figure 11. Difference in Dissipation of Thermal Variance Created by the Submarine Wake in the Pre-existing Turbulence Regime



Difference in dissipation of thermal variance for the pre-existing turbulence regime. The y-axis displays a logarithmic plot of the difference between  $\chi_{wake}$  and  $\chi_{ambient}$  in  $^{\circ}\text{C s}^{-1}$ . X-axis is measured in hours.  $R_p$  of 1.5, 2.0 2.5 are shown in black, blue and red, respectively. The horizontal black dashed line displays the detection threshold

## IV. DISCUSSION

### A. FLUID REGIME EFFECTS

This study presents a comparative analysis of the dissipation of turbulent kinetic energy and thermal variance in a stratified wake for three environmental regimes: (i) quiescent regime, (ii) double-diffusive regime, and (iii) a flow with pre-existing turbulence. As expected, the longest detection periods were observed for the quiescent case. The addition of pre-existing turbulence had a small effect on the overall structure of microstructure and slightly reduced wake duration. The mean time until  $\varepsilon$  dissipated below the detection threshold for the quiescent and turbulent regimes was 1.0442 and 0.8789 hours, respectively. The two regimes only differed by 0.1653 hours (~10 minutes). Since the magnitude of the initial perturbation was small compared to the magnitude of the wake forces, it had minimal impact on the wake duration. The double diffusion regime, however, showed a substantial decrease in wake duration. The mean time to the detection threshold of the double-diffusive regime, 0.5412 hours, was approximately half that of the quiescent regime. The shorter wake indicates that active double-diffusive convection does influence the physics of the wake turbulence. A possible explanation is that the centimeter scale forces of salt fingers are on a similar scale to the dissipation scale of both thermal variance and kinetic energy. That variable distribution of density further inhibits the vertical motion of the wake.

Even with the high resolution of this DNS, the verification of the exact mechanism for the decreased duration of the submarine wake in the presence of double diffusion is difficult. What is certain is that the turbulent microstructure created by a submarine wake is a viable method for detection and the kinetic energy is a longer lasting measure than thermal variance.

### B. DENSITY RATIO EFFECTS

The results of the numerical simulation do not yield a clear correlation between density ratios and wake duration across all regimes and in terms of  $\varepsilon$  and  $\chi$ . At the detection threshold there is minimal influence of the density ratio on the wake duration,

but small variations do occur especially toward the total dissipation time. There is variability between duration calculated using  $\varepsilon$  or  $\chi$ , and between fluid regimes. There were noticeable changes in wake duration as a function of density ratio. One clear trend in both  $\varepsilon$  and  $\chi$  and in all three fluid regimes was the wake generated with  $R_\rho = 2.5$  persisted the longest. The density ratio effects for  $\varepsilon$  were relatively similar across the three regimes. Both in the quiescent and double-diffusive regimes  $R_\rho = 2.0$  was the first below the threshold value, but in the turbulent regime  $R_\rho = 1.5$  was the first below the detection threshold. In  $\varepsilon$  the largest difference between any two density ratios across all three fluid regimes was .3663 hours (~22 minutes). Given that 1.233 hours was the longest duration of any wake, a 30% difference in duration is significant.

The practical utilization of the microstructure-based detection method is limited by time scales of wake duration. The relatively short detection periods obtained in this study are the product of a relatively small object, moving at slow speed and moderately high Reynolds number. A simple scale analysis presented below provides more insight into the potential for detection of real-world objects.

### C. REAL-WORLD ESTIMATES

The scaling of kinetic energy dissipation is shown in Equation (1), where  $U$  is the velocity scale of the submarine and  $L$  is the size scale. Based on dimensional analysis, the maximal kinetic energy dissipation ( $\varepsilon_0$ ) is expressed as a function of  $L$  and  $U$  as follows:

$$\varepsilon_0 = C \frac{U^3}{L}, \quad (1)$$

where  $C$  is a non-dimensional constant.

Assuming the dissipation rate is controlled by the environment and thus is independent of the submarine scale and velocity, the kinetic energy dissipation is expressed as a function of the initial  $\varepsilon_0$ , the time,  $t$ ; and the dissipation rate  $\lambda$ :

$$\varepsilon = \varepsilon_0 \exp(\lambda t) \quad (2)$$

Combining (1) and (2), we obtain the timescale ( $\Delta t$ ) required for  $\varepsilon$  to reach the threshold value ( $\varepsilon_{th}$ ):

$$\Delta t = \frac{1}{\lambda} \ln \left( \frac{\varepsilon_{th} L}{C U^3} \right). \quad (3)$$

An estimate of the persistence of a wake from a larger faster moving sub was made as follows. The data obtained from the shortest double-diffusive simulation ( $R_p=2.0$ ) yielded,  $\lambda = -4.025 \times 10^{-3}$  from an exponential best-fit curve. For the same experiment, the values of C was evaluated using (1), resulting in  $C = 2 \times 10^{-2}$ . This made it possible to make a conservative estimate of the detection period using (3) for arbitrary object sizes (L) and velocities (U). For instance, when U is increased to  $\sim 1$  m and L is increased to  $10 \sim$  m/s and the detection threshold still set to  $10^{-11}$ , Equation (3) indicates that the wake would be detectable for approximately two hours. Increased speed or object size would further increase the duration of detectable wake and in the future improved measurements could further expand those detections.

#### D. CONCLUSIONS

Numerical experiments regarding the persistence of submarine wakes in stratified fluids were performed. The influences of environmental conditions (quiescent, double diffusive and turbulent) and background density ratio were measured. The presence of double diffusion appeared to shorten the wake duration, but the precise physical mechanisms that caused this require higher-resolution modeling and further analysis. The resulting data indicated that there was marginal sensitivity to the background density ratio. The density ratio had some influence, especially at higher values of  $R_p$ , but the differences were on the orders of minutes. The wake signatures in terms of the kinetic energy dissipation were found to be more persistent than those based on thermal variance. Therefore, it is suggested that future experimental and modeling studies be focused on  $\varepsilon$  - based detection.

Overall, the current project revealed that microstructure-based detection, especially based on the dissipation of kinetic energy, is a viable operational method for

the detection of submerged moving objects. High-resolution numerical simulations can offer valuable guidance for implementation of such techniques.

## LIST OF REFERENCES

- Adcroft, A., C. Hill, J.-M. Campin, J. Marshall, and P. Heimbach, 2004: Overview of the formulation and numerics of the MIT GCM. *Seminar on Recent Developments in Numerical Methods for Atmospheric and Ocean Modeling*, 6–10 September 2004. Shinfield Park, Reading, ECMWF, 139–150.
- Ball, J., 2015: Double-Diffusive Convection in Rotational Shear. Thesis, Dept. of Oceanography, Naval Postgraduate School, 73 pp.
- Brucker, K. A., and S. Sarkar, 2010: A comparative study of self-propelled and towed wakes in a stratified fluid. *J. Fluid Mech.*, **652**, 373–404, doi:10.1017/S0022112010000236.
- Clyne, J., P. Mininni, A. Norton, and M. Rast, 2007: Interactive desktop analysis of high resolution simulations: Application to turbulent plume dynamics and current sheet formation. *New J. Phys.*, **9**, 301–301, doi:10.1088/1367-2630/9/8/301.
- de Stadler, M. B., and S. Sarkar, 2011: Simulation of a propelled wake with moderate excess momentum in a stratified fluid. *J. Fluid Mech.*, **692**, 28–52, doi:10.1017/jfm.2011.489.
- Ecke, R., 2005: The Turbulence Problem. *Los Alamos Sci.*, 124–141, doi:10.1007/978-94-007-0117-5.
- Lin, J. T., and Y. H. Pao, 1979: Wakes in Stratified Fluids. *Annu. Rev. Fluid Mech.*, **11**, 317–338, doi:10.1146/annurev.fl.11.010179.001533.
- Marshall, J., C. Hill, L. Perelman, and A. Adcroft, 1997: Hydrostatic, quasi-hydrostatic, and nonhydrostatic ocean modeling. *J. Geophys. Res.*, **102**, 5733, doi:10.1029/96JC02776.
- Peterson, A. K., and I. Fer, 2014: Dissipation measurements using temperature microstructure from an underwater glider. *Methods Oceanogr.*, **10**, 44–69, doi:10.1016/j.mio.2014.05.002.
- Radko, T., 2013: *Double-Diffusive Convection*. Cambridge University Press, 344 pp.
- Radko, T., A. Bulters, J. D. Flanagan, and J. M. Campin, 2014: Double-Diffusive Recipes. Part I: Large-Scale Dynamics of Thermohaline Staircases. *J. Phys. Oceanogr.*, **44**, 1269–1284, doi:10.1175/JPO-D-13-0155.1. <http://journals.ametsoc.org/doi/abs/10.1175/JPO-D-13-0155.1>.

- Richardson, L. F., 1926: Atmospheric diffusion shown on a distance-neighbor graph. *Proc. R. Soc. London. Ser. A, Contain. Pap. a Math. Phys. Character*, **110**, 709–737.
- Schmitt, R. W., 1994: Double diffusion in oceanography. *Annu. Rev. Fluid Mech.*, 26, 255–285.
- You, Y., 2002: A global ocean climatological atlas of the Turner angle: Implications for double-diffusion and water mass structure. *Deep-Sea Res.*, **49**, 2075–2093.

## **INITIAL DISTRIBUTION LIST**

1. Defense Technical Information Center  
Ft. Belvoir, Virginia
2. Dudley Knox Library  
Naval Postgraduate School  
Monterey, California